Journal of Inorganic Biochemistry 195 (2019) 1–12

Contents lists available at ScienceDirect

Journal of Inorganic Biochemistry

journal homepage: www.elsevier.com/locate/jinorgbio

Increased ROS generation causes apoptosis-like death: Mechanistic insights into the anti-*Leishmania* activity of a potent ruthenium(II) complex

Mônica Soares Costa[a], Yasmim Garcia Gonçalves[b], Samuel Cota Teixeira[c], Débora Cristina de Oliveira Nunes[a], Daiana Silva Lopes[a,d], Claudio Vieira da Silva[c], Marcelo Santos da Silva[e], Bruna Cristina Borges[f], Marcelo José Barbosa Silva[f], Renata Santos Rodrigues[a], Veridiana de Melo Rodrigues[a], Gustavo Von Poelhsitz[b], Kelly Aparecida Geraldo Yoneyama[a,*]

[a] *Laboratório de Bioquímica e Toxinas Animais, Instituto de Biotecnologia, Universidade Federal de Uberlândia, UFU, Uberlândia, MG, Brazil*
[b] *Instituto de Química, Universidade Federal de Uberlândia, UFU, Uberlândia, MG, Brazil*
[c] *Laboratório de Tripanosomatídeos, Instituto de Ciências Biomédicas, Universidade Federal de Uberlândia, UFU, Uberlândia, MG, Brazil*
[d] *Instituto Multidisciplinar em Saúde, Universidade Federal da Bahia, Campus Anísio Teixeira, Vitória da Conquista, Brazil*
[e] *Laboratório Especial de Ciclo Celular (LECC), Centro de Toxinas, Resposta imune e Sinalização Celular (CeTICS), Instituto Butantan, Universidade de São Paulo, USP, São Paulo, Brazil*
[f] *Laboratório de Osteoimunologia e Imunologia dos Tumores, Instituto de Ciências Biomédicas, Universidade Federal de Uberlândia, UFU, Uberlândia, MG, Brazil*

ARTICLE INFO

Keywords:
Ruthenium(II) complex
Leishmania (*Leishmania*) *amazonensis*
Cell death
Apoptosis
ROS production

ABSTRACT

Some metallodrugs that exhibit interesting biological activity contain transition metals such as ruthenium, and have been extensively exploited because of their antiparasitic potential. In previous study, we reported the remarkable anti-*Leishmania* activity of precursor *cis*-[$Ru^{II}Cl_2(dppm)_2$], where dppm = bis(diphenylphosphino) methane, and new ruthenium(II) complexes, *cis*-[$Ru^{II}(\eta^2\text{-}O_2CC_{10}H_{13})(dppm)_2]PF_6$ (bbato), *cis*-[$Ru^{II}(\eta^2\text{-}O_2CC_7H_7S)(dppm)^2]PF^6$ (mtbato) and *cis*-[$Ru^{II}(\eta^2\text{-}O_2CC_7H_7O_2)(dppm)_2]PF_6$ (hmxbato) against some *Leishmania* species. In view of the promising activity of the hmxbato complex against *Leishmania* (*Leishmania*) *amazonensis* promastigotes, the present work investigated the possible parasite death mechanism involved in the action of this hmxbato and its precursor. We report, for the first time, that hmxbato and precursor promoted an increase in reactive oxygen species production, depolarization of the mitochondrial membrane, DNA fragmentation, formation of a pre-apoptotic peak, alterations in parasite morphology and formation of autophagic vacuoles. Taken together, our results suggest that these ruthenium complexes cause parasite death by apoptosis. Thus, this work provides relevant knowledge on the activity of ruthenium(II) complexes against *L.* (*L.*) *amazonensis*. Such information will be essential for the exploitation of these complexes as future candidates for cutaneous leishmaniasis treatment.

1. Introduction

Protozoan parasites from more than 21 species of the *Leishmania* genus cause a group of diseases known as leishmaniasis, which present 4 main clinical manifestations: visceral leishmaniasis (VL, also known as kala-azar); post-kala-azar dermal leishmaniasis (PKDL); cutaneous leishmaniasis (CL); and mucocutaneous leishmaniasis (MCL). These different types of the diseases are present in 98 countries worldwide and the cutaneous leishmaniasis is the most common form. The World Health Organization (WHO) considers CL to be an emerging and uncontrolled disease, occurring mainly in tropical and subtropical regions. Additionally, the presence of 200,000 new cases only in the year 2015 was reported by the same agency [1,2].

Current treatments for leishmaniasis present limited efficacy, besides being associated with some limitations such as high cost, difficulties in drug administration, moderate toxicity and occurrence of parasitic resistance [3,4]. Moreover, there is still no effective vaccine against the disease [5]. Thus, it becomes evident that new therapeutic strategies must be developed against leishmaniasis.

Metallic complexes have been investigated as molecules for use as therapeutic agents [6,7]. Among these, the ruthenium complexes have been highlighted mainly due to their chemical characteristics and

* Corresponding author at: Pará avenue, 1720, CEP: 38400-902 Uberlândia, MG, Brazil.
E-mail address: kelly.tudini@ufu.br (K.A.G. Yoneyama).

https://doi.org/10.1016/j.jinorgbio.2019.03.005
Received 23 November 2018; Received in revised form 3 March 2019; Accepted 4 March 2019
Available online 06 March 2019
0162-0134/

biological applications, such as antitumor [8–10] and antiparasitic activities [8,11,12]. The advantages associated with the use of ruthenium include: (i) possibility of coordination with target molecules due to its octahedral geometry, (ii) versatility of coordination promoted by the different stages of oxidation, (iii) slow ligand-exchange kinetics and (iv) participation in the transport of important therapeutic agents due to the possibility of interaction with proteins present in human blood, such as transferrin and albumin [13–16].

Considering the similarities between the metabolic pathways of trypanosomatids and tumor cells, besides the high replicability of both cells, ruthenium complexes with antitumor activities are being evaluated for their antiparasitic activity [17–19]. Some studies have shown that ruthenium complexes induced apoptotic and/or autophagic effects on different tumor cell lines [20–22]. Despite the investigation of death mechanisms in trypanosomatid protozoa such as *Trypanosoma cruzi* and *Leishmania* spp. are growing, little is known about the mechanisms induced by ruthenium complexes in these protozoa. Knowledge on the death mechanism involved in a drug's action would elucidate the cellular response, thus enabling the prospection of more effective therapeutic agents [23–24]. Despite this context, death mechanisms of the drugs currently available for leishmaniasis treatment are not yet fully understood.

Apoptosis in multicellular organisms is described as a series of biochemical processes that lead to controlled cellular self-destruction, being characterized mainly by rounding of the cell, condensation of the chromatin, fragmentation of the nucleus (karyorrhexis), loss of the mitochondrial membrane potential ($\Delta\Psi_m$) and blebbing of the plasma membrane [24,25]. Although apoptosis has been described for the first time in these organisms, experimental evidence shows that similar mechanisms are present in trypanosomatids given that these parasites also presented a basic machinery to carry out this death type [26–29].

In a previous study developed by our research group showed that three new

ruthenium(II) complexes, *cis*-[$Ru^{II}(\eta^2$-$O_2CC_{10}H_{13})(dppm)_2]PF_6$ (bbato), *cis*-[$Ru^{II}(\eta^2$-$O_2CC_7H_7S)(dppm)_2]PF_6$ (mtbato) and *cis*-[$Ru^{II}(\eta^2$-$O_2CC_7H_7O_2)(dppm)_2]PF_6$ (hmxbato) derived from the precursor complex (*cis*-[$Ru^{II}Cl_2(dppm)_2$], where dppm = bis(diphenylphosphino)methane caused significant reductions in viabilities of *Leishmania* (*Leishmania*) *amazonensis*, *Leishmania* (*Viannia*) *braziliensis* and *Leishmania* (*Leishmania*) *infantum* promastigotes. Moreover, these complexes promoted expressive inhibitions of parasite infectivity in murine macrophage (RAW 264.7) [12]. Therefore, in view of the promising results previously obtained and the remarkable anti-*Leishmania* activity of the hmxbato complex against *L.* (*L.*) *amazonensis* promastigotes, the complex was selected for the present study. This paper describes through different assays the probable cell death mechanism involved in the action of ruthenium(II) complexes (precursor and hmxbato) against these parasites.

2. Material and methods

2.1. Chemicals

Dimethyl sulfoxide (DMSO), penicillin, streptomycin, Rhodamine 123 (Rh 123), monodansylcadaverine (MDC) and glutamine were purchased from Sigma Chemical Co. (St. Louis, USA) and heat-inactivated fetal bovine serum (FBS) from Cultilab (São Paulo, Brazil). All other reagents were of analytical or superior grade.

2.2. Synthesis of ruthenium(II) complexes

The precursor complex was synthesized as described in the literature [30], whereas hmxbato was synthesized and purified by appropriate chemical methods as previously described [12]. Ruthenium complexes were dissolved in DMSO to obtain a 10 mM stock solution of complex and stored at 4 °C. For experiments, new dilutions were prepared in culture medium to ensure that the DMSO concentration in culture medium did not exceed 0.1%. Concentrations of complexes used in assays were based on the concentration that is cytotoxic to 50% of promastigotes (IC_{50}) as previously described [12].

2.3. Promastigote culture

L. (*L.*) *amazonensis* (IFLA/BR/67/PH8 strain) promastigotes were cultured in liver infusion tryptose (LIT) medium, pH 7.4, supplemented with 10% FBS, 1% penicillin (10,000 UI·mL^{-1}) and streptomycin (10 mg·mL^{-1}), 2% glucose – complete LIT - at 23 ± 0.5 °C. Promastigotes used in all experiments were isolated from the stationary growth phase.

2.4. Antiproliferative assay

In order to evaluate the effects of hmxbato and precursor on the proliferation of *L.* (*L.*) *amazonensis* promastigotes, parasites (5×10^6 cells·mL^{-1}) were cultured in 25 cm^2 cell culture flasks containing complete LIT in the absence (control) or presence of hmxbato or precursor at respective concentrations of 0.52 μM and 15.48 μM (IC_{50} values). The promastigote concentrations were monitored at times of 6, 12, 24, 48 and 72 h after fixation of parasites with 1% paraformaldehyde in cacodylate buffer and blind counts in a Neubauer Chamber. This assay was carried out in triplicate and three independent experiments were performed.

2.5. Cell cycle analysis

Promastigotes (5×10^6 cells·mL^{-1}) were incubated for 24 h in the absence (control) or presence of hmxbato (IC_{50}) or precursor (IC_{50}). After incubation, parasites were washed in phosphate buffered saline (PBS) and resuspended in a solution of 70% ice-cold ethanol in PBS and fixed for 18 h at 4 °C. Subsequently, the parasites were incubated with 10 μg·mL^{-1} propidium iodide (PI) and 100 μg·mL^{-1} RNAse A in PBS for 45 min at 37 °C under light protection. The cell population analyses were performed with a flow cytometer (FACSCanto II, BD); a total of 10,000 events were acquired in the region previously established as corresponding to parasites. The software FlowJo was employed to analyze the parasite percentages in each cell cycle phase: sub-G1, G1, S and G2-M.

2.6. Analysis of DNA fragmentation by the TUNEL assay

To detect in situ DNA fragmentation, the terminal deoxynucleotidyl transferase dUTP nick end labeling (TUNEL) technique was carried out by the Apoptosis Detection System, Fluorescein kit (Promega). Briefly, promastigotes (5×10^6), cultured in the absence (control) or presence of hmxbato (IC_{50}) or precursor (IC_{50}) for 24 h, were washed in PBS and fixed with 1% paraformaldehyde in cacodylate buffer for 15 min. Fixed cells were washed with PBS and permeabilized by the addition of 0.1% Triton X-100 for 5 min at 25 °C; the TUNEL assay was performed according to the manufacturer's protocol. VECTASHIELD® Mounting Medium with 4,6′-diamidino-2-phenylindole dilactate (DAPI) (Vector Labs) was added to serve as an anti-fade mounting solution and to stain nuclear DNA. Negative and positive controls were the internal controls of the assay. For negative control, TUNEL reaction was carried out without TdT enzyme. For positive control, parasites were pretreated with 1 unit·mL^{-1} of DNase I for 10 min. Cells were analyzed using an Olympus Bx51 fluorescent microscope (100× oil objective) attached to an EXFO Xcite series 120Q lamp and a digital Olympus XM10 camera with the camera controller software Olympus Cell F (Olympus, Japan). Fluorescent images were obtained via the software Olympus - Cell F.

2.7. Evaluation of mitochondrial damage ($\Delta\Psi_m$)

Rhodamine 123 (Rh 123), a specific fluorescent dye that accumulates within active mitochondria, was used to assess mitochondrial membrane potential ($\Delta\Psi_m$) of promastigotes. Parasites (5×10^6 cells·mL^{-1}) cultured in the absence (control) or presence of hmxbato (IC_{50}) or precursor (IC_{50}) for 24 and 48 h were incubated with Rh 123 (15 µg·mL^{-1}) for 15 min at 25 °C under light protection. Subsequently, the parasites were washed in PBS, fixed with 1% paraformaldehyde in cacodylate buffer and washed again in PBS. The cell population analysis was performed in a flow cytometer (FACSCanto II, BD); a total of 10,000 events were acquired in the region previously established as corresponding to the parasites. This assay was performed in triplicate and the data shown in the graphs represent the average values. The software FlowJo was employed to analyze the fluorescence intensity. Alternatively, parasites incubated with Rh 123 were observed in a confocal microscope (Zeiss LSM510 Meta) and captured images were processed using the software Adobe Photoshop 5.5 (Adobe Systems, Inc., Mountain View, CA, USA).

2.8. Measurement of reactive oxygen species

To quantify the reactive oxygen species (ROS) production, promastigotes (5×10^6 cells·mL^{-1}) cultured in the absence (control) or presence of hmxbato (IC_{50}) or precursor (IC_{50}) for 24 h were collected by centrifugation at 2500*g* for 5 min, washed in PBS and incubated with 2 µM 5-(and-6)-chloromethyl-2′,7′dichlorodihydrofluorescein diacetate acetyl ester (CM-H_2DCFDA) (Invitrogen) for 30 min at 23 ± 0.5 °C. For this assay 10,000 cells were analyzed in each group (control and treated) using a BD FACSCanto II flow cytometer (BD Biosciences). The fluorescence was measured and represented by histogram (counts × FL1-A). The software FlowJo was utilized to analyze the fluorescence intensity. This assay was performed in triplicate and the values shown in the graphs represent the average values.

2.9. Cellular morphology and ultrastructure of L. (L.) amazonensis promastigotes

L (*L.*) *amazonensis* promastigotes (5×10^6·mL^{-1}) were cultured in the absence (control) or presence of hmxbato (IC_{50}) or precursor (IC_{50}) at 23 ± 0.5 °C for 24 h. The parasites were washed in PBS, fixed with 1% paraformaldehyde in cacodylate buffer and resuspended in PBS (pH 7.4). The suspensions of fixed parasites were placed on glass coverslips and stained with 50 µg·mL^{-1} fluorescent phalloidin conjugate (phalloidin-Atto 565) and To-pro solution in PBS for 50 min at 25 °C in a humidified chamber according to the manufacturer's instructions. The cell morphology was analyzed in a confocal microscope (Zeiss LSM510 Meta) and captured images were processed using the software Adobe Photoshop 5.5 (Adobe Systems, Inc., Mountain View, CA, USA). Alternatively, the phalloidin fluorescence intensity and single-cell area were manually measured by the software ImageJ (National Institutes of Health, USA). For ultrastructural analysis, promastigotes were treated (hmxbato and precursor) or not (control) for 24 h. After incubation or not with complexes, parasites were fixed for 12 h at 4 °C in a solution containing 2.5% glutaraldehyde diluted in 0.1 M PBS, pH 7.2, washed in PBS and post-fixed for 1 h in a solution containing 1% osmium tetroxide (OsO_4) and 0.8% potassium ferrocyanide in PBS. The cells were washed in PBS, dehydrated in a graded acetone series and embedded in resin. Ultrathin sections were contrasted with uranyl acetate and lead citrate then observed under a transmission electron microscope (HITACHI HT7700).

2.10. Formation of autophagic vacuoles

The monodansylcadaverine (MDC) labeling was carried out to evaluate the formation of autophagic vacuoles. Promastigotes (5×10^6 cells·mL^{-1}) cultured in the absence (negative control) or presence of hmxbato (IC_{50}) or precursor (IC_{50}) for 24 h were incubated with 200 µM MDC for 1 h under light protection. Parasites treated with 1 µM Rottlerin for 24 h served as the positive control. In the next step, the parasites were washed in PBS, fixed with 1% paraformaldehyde in cacodylate buffer and washed again in PBS. Parasites were placed on glass coverslips for mounting on microscope slides and analyzed in a fluorescence microscope (Zeiss LSM510, Germany) at excitation wavelength 358 nm and emission wavelength 463 nm. The fluorescence intensity was quantified by the software ImageJ version 1.48.

2.11. Statistical analysis

Data are expressed as mean ± standard deviation of experiments performed at least three times in triplicate. All data were first checked for normal distribution. Significant differences were determined by one-way ANOVA and Tukey's multiple comparisons test (GraphPad Prism Software version 6.01). Data were considered statistically significant at $p < 0.05$ (*). Higher significance values $p < 0.01$ (**), $p < 0.001$ (***) and $p < 0.0001$ (****) are also indicated.

3. Results

3.1. Ruthenium(II) complexes induce antiproliferative effect on promastigotes

The treatment with precursor and hmxbato caused statistically significant reductions in the proliferation of *L.* (*L.*) *amazonensis* promastigotes when compared to the control (untreated group) (Fig. 1). The antiproliferative effect caused by the ruthenium complexes could be observed just after 6 h of cultivation, when reductions of approximately 36% ($p < 0.001$) and 45% ($p < 0.001$) were observed in parasite growth for the precursor and hmxbato, respectively. Expressive antiproliferative effects were observed throughout the parasite culture in

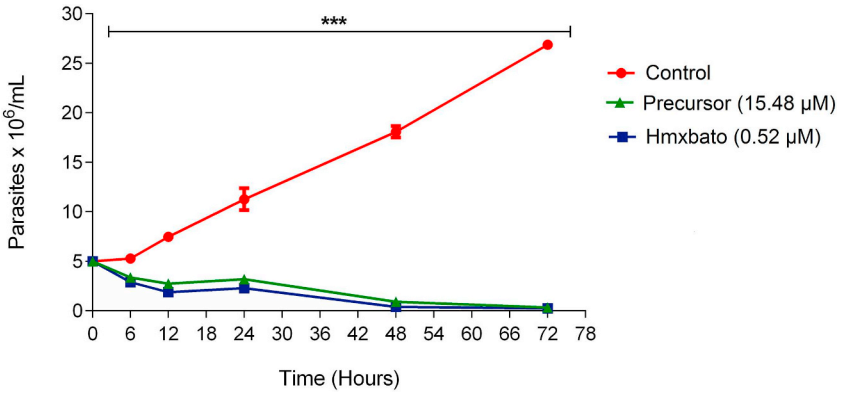

Fig. 1. Antiproliferative effect caused by ruthenium(II) complexes on *L.* (*L.*) *amazonensis* promastigotes. The concentration-response curves showed the parasite concentration in culture after 6, 12, 24, 48 and 72 h treatment with precursor and hmxbato. The promastigote concentrations were determined by direct counting of fixed cells in a Neubauer Chamber. The data are expressed as the means ± standard deviations of experiments performed in triplicate. Significant differences were determined using one-way ANOVA, Tukey's multiple comparisons test. Differences were regarded as higher significant when $p < 0.001$ (***).

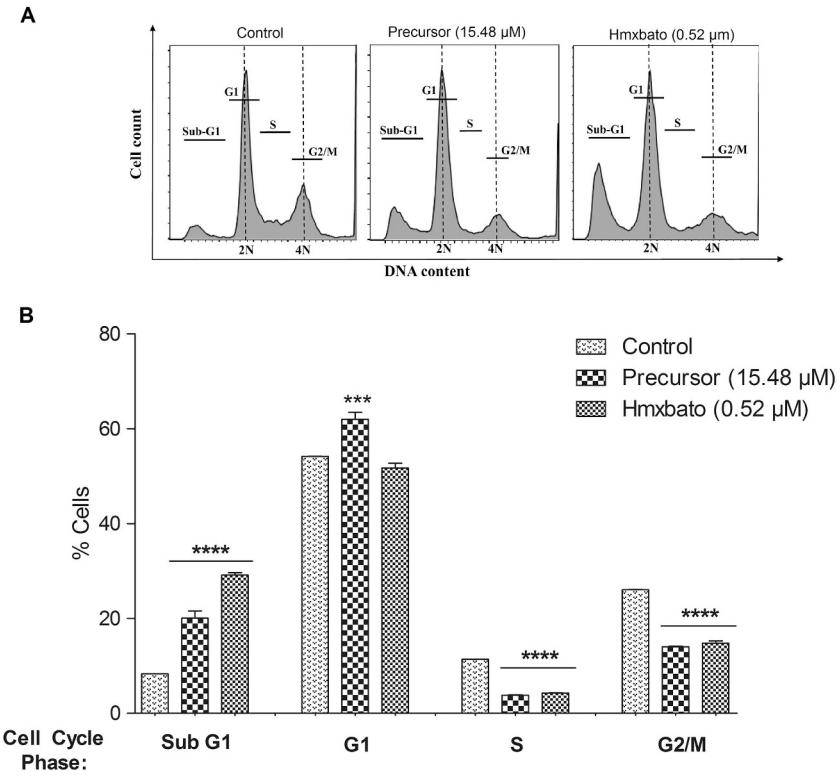

Fig. 2. Ruthenium(II) complexes caused a cell cycle arrest in the sub-G1 phase, followed by decreased of cells in the S and G2/M phases. *L.* (*L.*) *amazonensis* promastigotes were culture for 24 h in the absence (control) or presence of precursor (IC_{50}) or hmxbato (IC_{50}) and then submitted to cell-cycle analysis (**A**) The histograms show the distribution of cells according to parasite DNA content after staining with PI. The fluorescence was measured by flow cytometry. (**B**) The graph shows the percentages of cells from each subpopulation in the cell-cycle phases: sub-G1, G1, S, G2/M. The data are expressed as the means ± standard deviations of experiments performed in triplicate and in each replicate 10,000 cells were analyzed. Significant differences were determined using one-way ANOVA, Tukey's multiple comparisons test (**B**). Differences were regarded as highly significant when $p < 0.001$ (***) or $p < 0.0001$ (****).

the presence of ruthenium complexes. After 24 h, treated parasites showed a reduction in the promastigote concentration in culture medium, evidencing that there was no proliferation after this time. Control parasites, cultured in the absence of ruthenium complexes, exhibited exponential growth characteristic of normal parasites.

3.2. Ruthenium(II) complexes promote cell cycle alterations

In order to verify the effect of complexes on promastigote replication and confirm possible alterations in the cell cycle, control and treated parasites were incubated with PI and analyzed by flow cytometry (Fig. 2A, B). The results indicate that both precursor and hmxbato promoted alterations in the cell cycle when compared with control parasites, with statistically significant decrease in cell percentages being observed in the S phase (from 11.4 to 3.9 and 4.2%, respectively) and in the G2/M phase (from 26 to 14.1 and 14.8%, respectively). Remarkably, a significant percentage of hmxbato-treated cells and a lower percentage of precursor-treated cells were arrested in the sub-G1 phase (Fig. 2B).

3.3. Ruthenium(II) complexes cause DNA fragmentation

DNA fragmentation provides further evidence of death by apoptosis. Thus, to verify the effect of ruthenium complexes and their possible action on DNA fragmentation, we carried out the TUNEL assay. Fig. 3 shows representative fluorescence images of the parasites in different conditions analyzed: negative control (parasites in which TUNEL reaction was carried out without TdT enzyme), positive control (parasites pretreated with 1 unit·mL^{-1} of DNase I), control (parasites without treatment), precursor (parasites treated with precursor), and hmxbato (parasites treated with hmxbato). The DIC (differential interference contrast) column shows the contrast of the cells under white-light exposure, which evidences the altered morphology after precursor and hmxbato treatments. The merged column shows the overlay between DAPI (used to stain DNA) and DNA frag (used to capture green fluorescence emitted by TUNEL-positive cells, which represents the DNA fragmentation). The white dashed squares highlight representative cells from each condition, while their decomposition (in DAPI and DNA frag) is represented on the right side of the figure. The green fluorescence exhibited by promastigotes treated with precursor or hmxbato, as well as the fluorescence presented by the positive control (+ DNase I), indicated strong DNA fragmentation in treated parasites. Furthermore, it was observed that the hmxbato caused a more high DNA fragmentation when compared to the precursor, given that the fluorescence images of parasites treated with hmxbato did not show the organelles containing well defined DNA (nucleus and kinetoplast). Of note, the DNA fragmentation was so intense that it was not possible to quantify the percentage of cells showing DNA fragmentation treated with hmxbato or its precursor.

3.4. Ruthenium(II) complexes cause a marked change in mitochondrial membrane potential ($\Delta\Psi_m$)

Parasites of the *Leishmania* genus present a single mitochondrion, which is essential to ensure their survival. Therefore, changes in the mitochondrial potential may imply in the activation of intrinsic apoptotic pathways [31,32]. In order to verify the effect of complexes on $\Delta\Psi_m$, control and treated promastigotes were stained with Rh 123, a fluorescent dye that accumulates inside mitochondria with polarized membrane, resulting in a fluorescence emission. Analysis by fluorescence microscopy revealed that after 24 h both precursor and hmxbato caused a decreased in Rh 123 fluorescence (Fig. 4A, panels F and J). Flow cytometry analysis performed after 24 h also showed significant reductions in Rh 123 fluorescence intensity for treated parasites (Fig. 4B, 24 h). Taken together, these results indicate that ruthenium complexes cause mitochondrial membrane depolarization. This depolarization was even more pronounced after treatment with complexes for 48 h since no fluorescence was detected by microscopy (Fig. 4A, panels H and L). At this 48 h measurement, a discrete fluorescence was detected only by flow cytometric analysis. As expected, control parasites exhibited high fluorescence intensity at both 24 and 48 h (Fig. 4A, panels B and D; Fig. 4B).

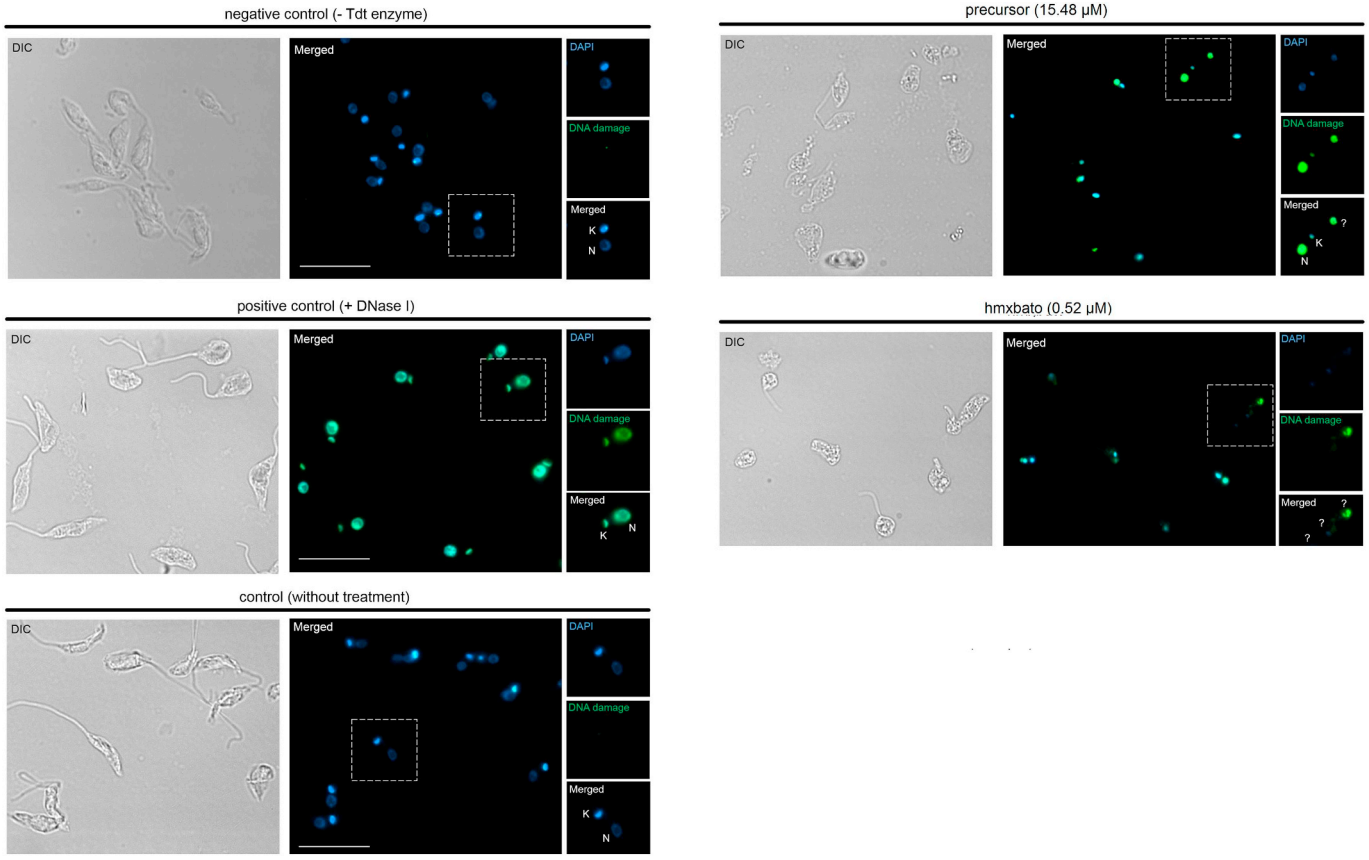

Fig. 3. Ruthenium(II) complexes induced DNA fragmentation of *L.* (*L.*) *amazonensis* promastigotes. *L.* (*L.*) *amazonensis* promastigotes were cultured for 24 h in the absence (control – without treatment) or presence of precursor (IC_{50}) or hmxbato (IC_{50}). Internal controls of the assay were included [negative control (without Tdt enzyme) and positive control (pre-treated with DNase I)]. The TUNEL assay was performed as previously described in order to evaluate the DNA fragmentation. DIC column evidences the morphology of the cells. Merged column represents the overlay between DAPI-stained organelles (blue field) and DNA fragmentation (green field). The white dashed squares highlight cells representative of each condition and their decomposition (in DAPI and DNA frag) is present on the right side of the figure. This assay was carried out in triplicate. K = kinetoplast, N = nucleus, ? = undefined organelles. The bar corresponds to 10 μm. Merged images were generated using the software Olympus - cell F.

3.5. Ruthenium(II) complexes increase ROS production

Alterations in $\Delta\Psi_m$ may occur due to an increase of ROS production. Thus, in order to analyze the ROS production, control and treated parasites were incubated with CM-H_2DCFDA fluorescent dye and submitted to flow cytometry analysis. The software FlowJo was employed to analyze the parasite percentage positive for ROS. Both precursor and hmxbato, after 24 h of treatment, promoted an increase of parasite ROS levels when compared with control parasites (Fig. 5). The quantitative analysis of ROS-positive parasites performed according to the histogram result showed statistically significant increase ($p < 0.0001$) after treatment with precursor (21% positive cells) and hmxbato (42% positive cells) when compared to the control (8% positive cells) (Fig. 5B).

3.6. Ruthenium(II) complexes drastically alter the promastigote morphology

Alterations in cell morphology may generate important additional information regarding the effects of a treatment on the parasite. Thus, promastigotes cultured for 24 h with ruthenium complexes were stained with fluorescent phalloidin conjugate and To-pro and submitted to morphological analysis by confocal microscopy. Both precursor and hmxbato promoted changes in parasite morphology (Fig. 6A). However, more pronounced alterations were observed after treatment with hmxbato (Fig. 7, panels E and F), as follows: (1) rounding of the promastigote body (indicated by white arrows), (2) loss of cell volume and (3) alteration in number of flagella (indicated by black arrows) and (4) altered pattern of actin polymerization. Additionally, the fluorescence intensity of phalloidin and the area of the parasite were quantified by the software Image J. Our results showed that both the precursor and hmxbato led to a hyperpolarization of actin filaments (Fig. 6B) in addition to a decrease in the parasite area (Fig. 6C). These changes were more pronounced for hmxbato than precursor. Ultrastructural analysis revealed more details about the damage that the treatment promoted in parasites. Drastic alterations were observed (Fig. 7), such as: pronounced mitochondrial swelling, alteration in chromatin condensation pattern/DNA fragmentation, presence of lipid bodies and acidocalcisomes, vacuolization and blebbing in the membrane (precursor). For hmxbato, the same changes were observed, but with the addition of more acidocalcisomes. In both treatments, not only did the kinetoplast remain intact, but also the cell membrane continued to present subpellicular microtubules.

3.7. Ruthenium(II) complexes induce the formation of autophagic vacuoles

Control and treated parasites were incubated with MDC, a fluorescent dye that is able to detect the presence of autophagic vacuoles. Both precursor and hmxbato induced the formation of autophagic vacuoles in parasites (Fig. 8A). As expected, control parasites did not exhibit fluorescence whereas parasites treated with Rottlerin, an autophagy inducer, showed fluorescence. The quantification of MDC fluorescence intensity showed that hmxbato produced a more intense effect on the parasite when compared with the precursor. However, both precursor and hmxbato promoted statistically significant increases in the MDC fluorescence intensity when compared to control parasites

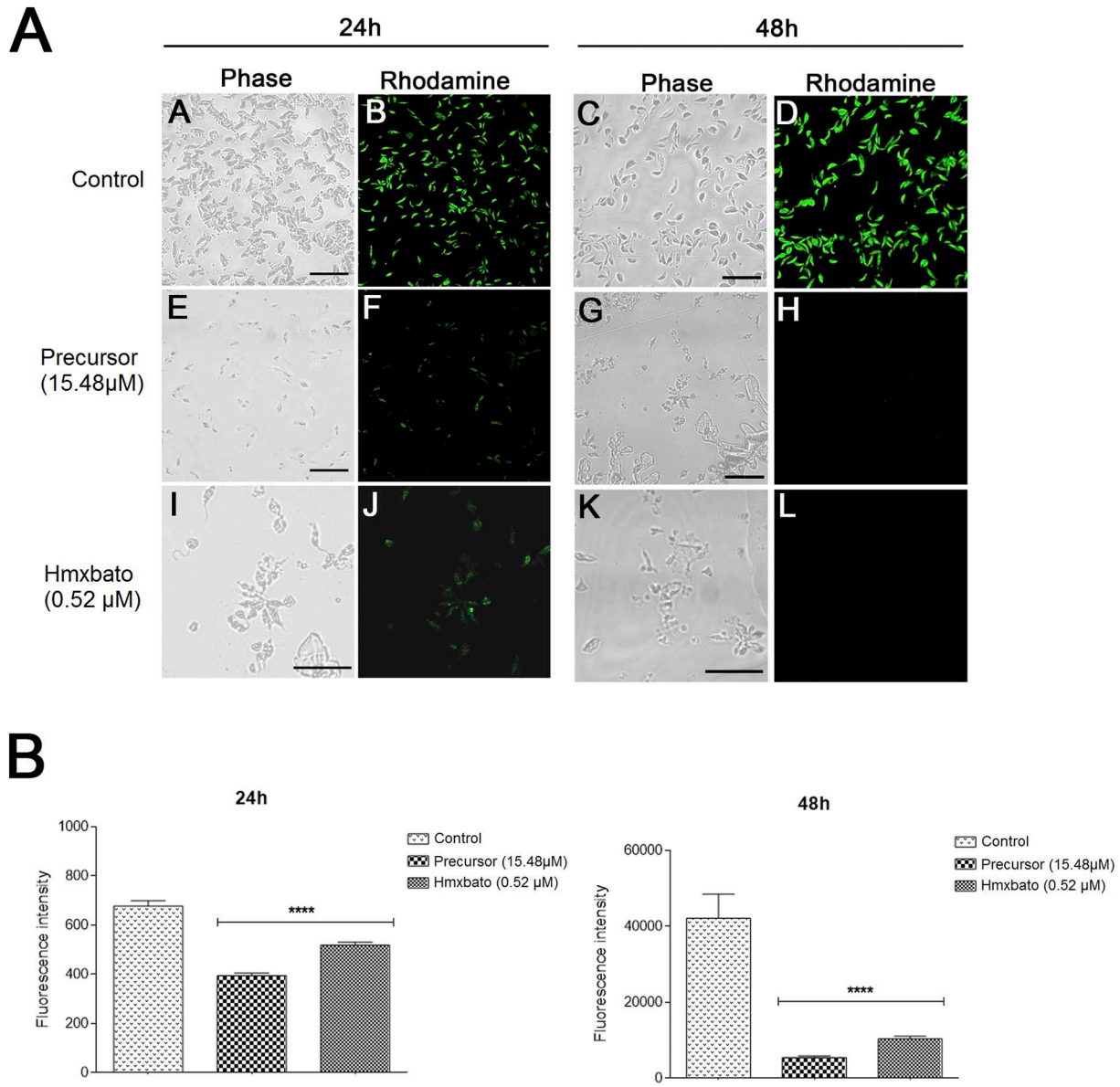

Fig. 4. Mitochondrial damage induced by hmxbato or precursor against *L.* (*L.*) *amazonensis* promastigotes. (**A**) Images obtained by confocal microscopy showing parasites cultured in the absence (control, panels A–D) or presence of precursor (IC_{50} – panels E–H) or hmxbato (IC_{50} – panels I–L) for 24 h or 48 h and submitted to staining with Rhodamine 123 for detection of mitochondrial membrane potential ($\Delta\Psi_m$). The depolarization of mitochondrial potential is represented by the decrease of green fluorescence. Bars: 20 μm. (**B**) Alternatively, parasites submitted to the same treatments described above were used for fluorescence intensity quantification emitted by flow cytometry. The data are expressed as the means ± standard deviations of experiments performed in triplicate and 10,000 cells were analyzed in each replicate. Significant differences were determined using one-way ANOVA, Tukey's multiple comparisons test (**B**). Differences were regarded as highly significant when $p < 0.0001$ (****).

(Fig. 8B).

3.8. Potential death mechanisms induced by ruthenium complexes

Our results suggest that the ruthenium complexes may be acting as oxidizing agents that lead to increased ROS generation in the *Leishmania* parasite. The ROS level elevation generated a cell stress that would induce the effects described below: (1) depolarization in $\Delta\Psi_m$, as revealed by the decrease in Rh123 dye; (2) DNA cleavage, as observed by the TUNEL assay and detection of pre-apoptotic peak by the cell cycle analysis; (3) alterations in the parasite morphology which began to show a rounded shape, loss in cell volume and altered pattern of actin polymerization; (4) formation of autophagic vacuoles, as detected by MDC labeling, through which the parasite attempts to remodel and fight against the stress generated. Taken together, these findings on the effect of ruthenium complexes against the *Leishmania* parasite lead us to propose a cytotoxic mechanism involving apoptosis-like death (Fig. 9).

4. Discussion

Leishmaniasis is a neglected disease whose current therapy still presents a series of disadvantages. Several studies have been carried out in order to discover new candidates for anti-*Leishmania* agents, which would contribute to improving the efficacy of the disease treatment [11,33–35]. In this sense, the metal complexes have been extensively exploited mainly due to their evidenced antiparasitic activity.

Our group has investigated some therapeutic alternatives for leishmaniasis treatment [12,36]. We report in a previous study the anti-*Leishmania* action of 3 new ruthenium complexes: bbato, mtbato and hmxbato, which promoted remarkable cytotoxic effects on *L.* (*L.*)

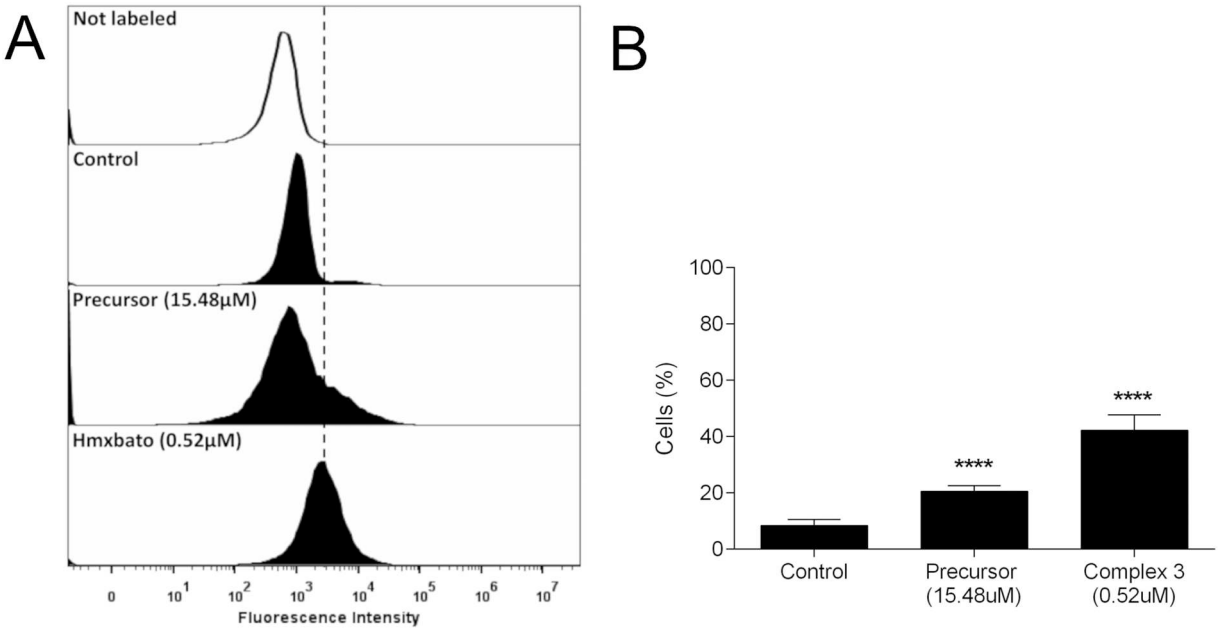

Fig. 5. CM-H_2DCFDA incorporation assay demonstrating an increase in intracellular reactive oxygen species (ROS) levels after treatment with ruthenium complexes. *L.* (*L.*) *amazonensis* promastigotes were cultured for 24 h in the absence (control) or presence of precursor (IC_{50}) or hmxbato (IC_{50}). (**A**) The histogram represents ROS levels produced by parasites after incubation with fluorescent dye CM-H_2DCFDA and analysis by flow cytometry. (**B**) The graph shows the percentage quantification of the ROS-positive cells in each treatment. The values exhibited in the graph were obtained from the histogram shown in (A). The assay was performed in triplicate and 10,000 cells were analyzed in each replicate. The results represent the average of three independent assays. Differences were regarded as highly significant when $p < 0.0001$ (****).

amazonensis, *L.* (*V.*) *braziliensis* and *L.* (*L.*) *infantum* promastigotes, showing IC_{50} values ranging from 12.59 to 0.52 μM, depending on the species analyzed. In addition, all ruthenium complexes significantly inhibited the parasite infection, yielding infectivity inhibition of up to 85%. The hmxbato was the most effective against three *Leishmania* species, mainly against *Leishmania* (*L.*) *amazonensis* promastigotes [12].

As to the results presented in this paper, the growth curve of the promastigote indicated that both hmxbato and precursor caused a strong antiproliferative effect with statistically significant inhibitions of parasite growth starting after 6 h of incubation with the complexes and extending until the end time of the assay. Verçoza et al. [28] recently demonstrated a similar antiproliferative effect after treatment of *L.* (*L.*) *amazonensis* promastigotes with 5 μM of KH-TFMDI (6,7-di-chloro-3-[4-(trifluoromethyl)benzylidene] indolin-2-one), a novel

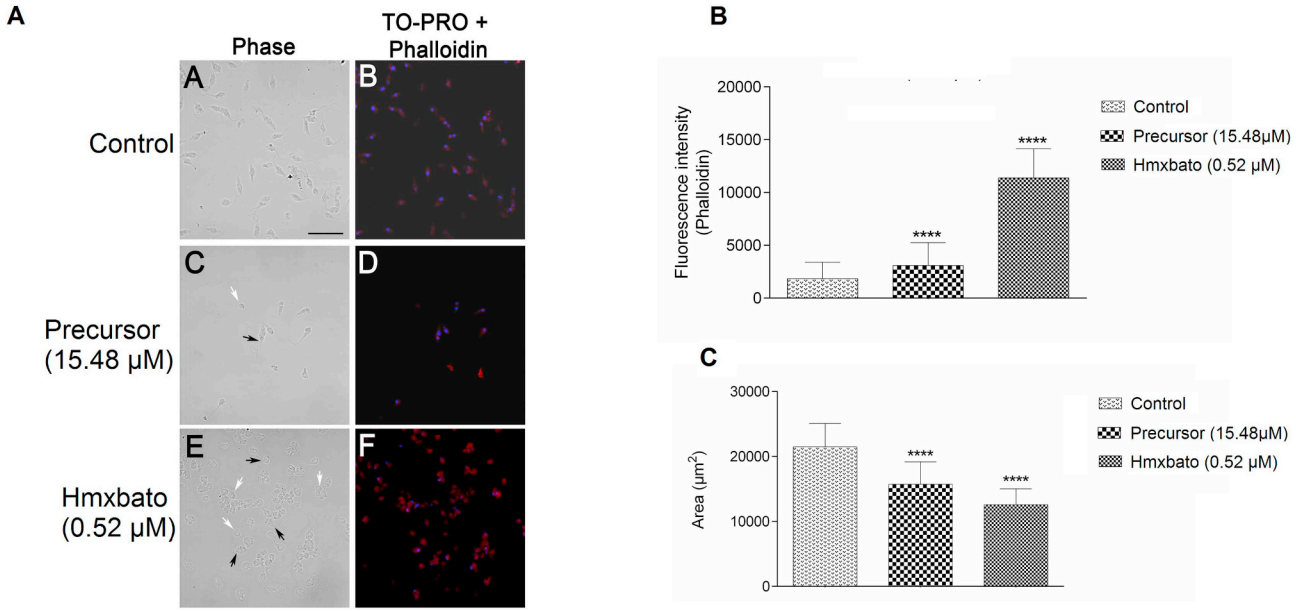

Fig. 6. Morphological changes caused by ruthenium(II) complexes in *L.* (*L.*) *amazonensis* promastigotes. *L.* (*L.*) *amazonensis* promastigotes were cultured for 24 h in the absence (control) or presence of precursor (IC_{50}) or hmxbato (IC_{50}) and then submitted to microscopic analysis. (**A**) Panels **A**, **C** and **E** showed contrast-phase of parasites. Panels **B**, **D** and **F** showed parasites stained with phalloidin and To-Pro. The white arrows indicate promastigotes with a rounded body. The black arrows indicate parasites with altered number of flagella. Images are representative of three independent experiments. Bars: 20 μm. (**B**) The graph shows the quantification of the fluorescence intensity of phalloidin and (**C**) the area of the parasite. The data are expressed as the means ± standard deviations of experiments performed in triplicate. Significant differences were determined using one-way ANOVA, Tukey's multiple comparisons test.

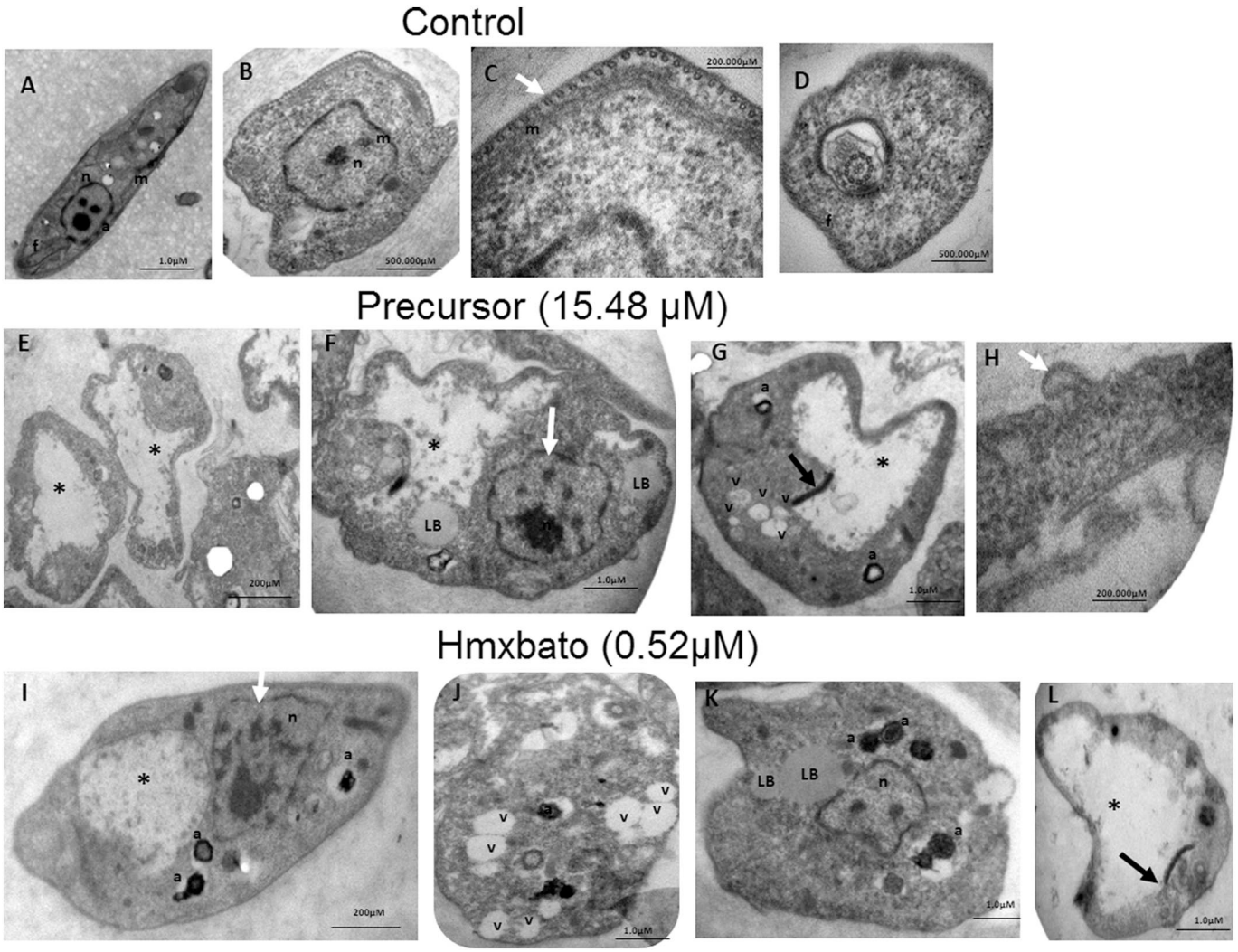

Fig. 7. Ultrastructural and morphological alterations observed in *L.* (*L.*) *amazonensis* promastigotes treated with ruthenium(II) complexes. Transmission electron microscopy (TEM): (**A–D**) control parasite: **A–B**. typical morphology with a single mitochondrion; **C**. intact membrane with subpellicular microtubules (white arrow); **D**. single flagellum. (**E–H)** Precursor-treated parasites: **E**. mitochondrial swelling (black asterisk); **F**. lipid bodies (LB), altered chromatin condensation pattern (white arrow); **G**. vacuolization, presence of acidocalcisomes and intact kinetoplast (black arrow); **H**. membrane blebbing (white arrow). (**I–L**). Hmxbato treated parasites: **I**. mitochondrial swelling (black asterisk); altered chromatin condensation pattern (white arrow) and presence of acidocalcisomes; **J**. intense vacuolization; **K**. lipid bodies (LB) and acidocalcisomes; **L**. mitochondrial swelling (black asterisk) and intact kinetoplast (black arrow). **a** = acidocalcisome; **m** = mitochondrion; **n** = nucleous; **v** = vacuole.

histone deacetylase inhibitor. Another study using six new transition metal complexes with a bioactive molecule (5,7-dimethyl-1,2,4-triazolo [1,5-*a*]pyrimidine - dmtp) acting against *L.* (*L.*) *infantum* and *L.* (*V.*) *braziliensis* promastigotes also revealed an antiproliferative effect. After 72 h of incubation, IC_{50} values were calculated and presented the following values: 27.7–97.7 μM and 10.0–45.1 μM against *L.* (*L.*) *infantum* and *L.* (*V.*) *braziliensis*, respectively [37].

In order to investigate whether the antiproliferative effect was correlated with interference in parasite cell division, the cell cycle assay was performed. The results indicated changes in the cell cycle profile, namely a percentage decrease of cells in the S phase and consequently in the G2/M phase. These cell-cycle alterations account for the action of ruthenium complexes on promastigote proliferation. Interestingly, the cell-cycle analysis also revealed that an expressive percentage of promastigotes were located on the left of the G1 phase (sub-G1 peak). In other words, a significant percentage of parasites did not enter the mitotic phase.

The percentage increase of cells in the sub-G1 phase and their decrease in the S phase may indicate that fragmentation in genomic DNA of promastigotes is so intense that it impairs their replication and thus leads to cell death [38]. Similar changes in the cell-cycle profile were observed in *L.* (*L.*) *amazonensis* promastigotes after their exposure not only to ruthenium-clotrimazole complexes ([(*p*-cymene)$RuCl_2$(CTZ)] – AM160 and [(*p*-cymene)RuCl(acac) (CTZ)]BF_4 (acac = acetylacetonate) – AM162) for 24 h, but also to acute oxidative stress. In these studies, the treatment promoted an increase and a decrease in the cell populations in the sub G0/G1 and S phases, respectively [39,40]. More recently, parasites of the same species treated with a vanadium complex ($[VO(C_{20}H_{16}N_4O_2]\cdot H_2O$ – VOSalophen, where Salophen = 4-acetamidofenil 2-hidroxibenzoato), also for a period of 24 h, showed the same cell-cycle profile [34].

DNA fragmentation is considered by some authors to be one of the markers used to indicate apoptosis-like death [24,41,42]. Thus, the DNA fragmentation of *L.* (*L.*) *amazonensis* promastigotes demonstrated herein motivated the search to elucidate the type of cell death involved in the action of ruthenium complexes. The DNA fragmentation analyzed by the TUNEL assay showed that both precursor and hmxbato caused DNA fragmentation after 24 h of treatment. The DNA damage was so expressive that, as commented previously, it was not possible to perform the quantification of damaged cells, since the most parasites

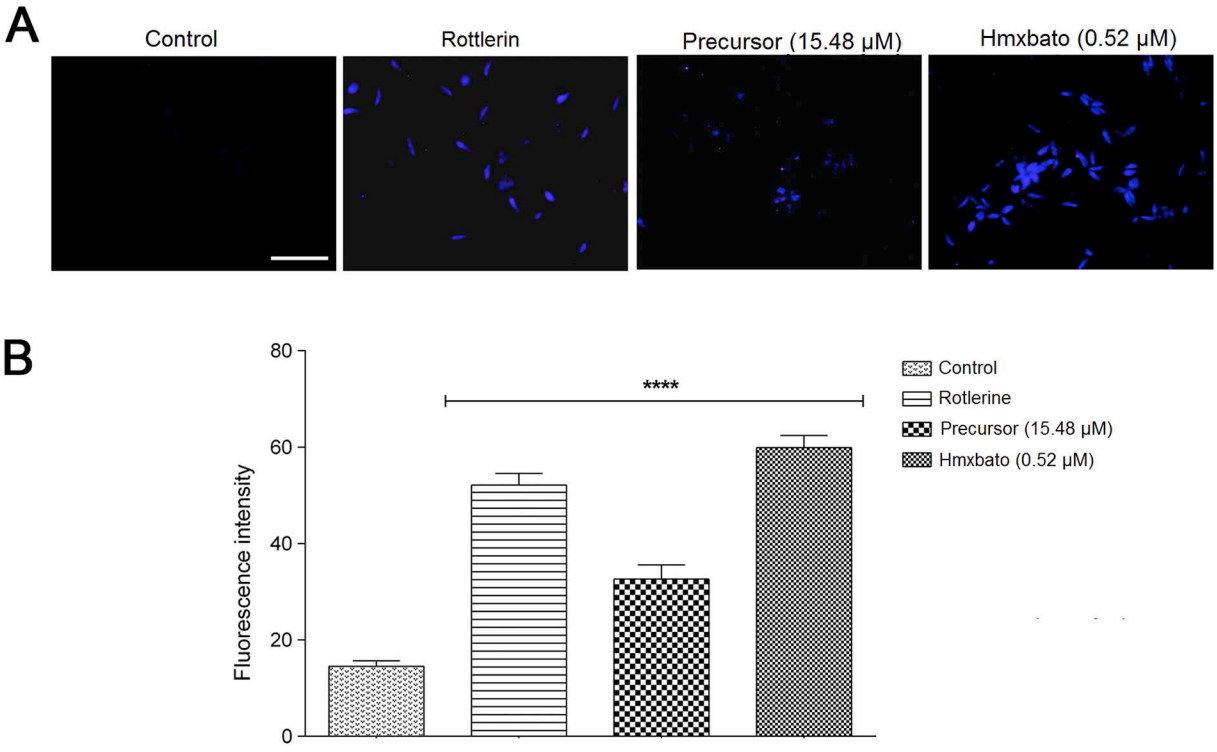

Fig. 8. Hmxbato and precursor induced the formation autophagic vacuoles in parasites. *L.* (*L.*) *amazonensis* promastigotes were cultured for 24 h in the absence (control) or presence of precursor (IC_{50}) or hmxbato (IC_{50}). (**A**) After treatments, the parasites were incubated with MDC reagent and analyzed in a fluorescence microscope (Zeiss LSM510, Germany) at excitation wavelength 358 nm and emission wavelength 463 nm. Parasites previously incubated with Rottlerin (autophagy inducer) are included as positive control. (**B**) The graph shows the quantification of fluorescence intensity in images obtained by fluorescence microscopy. The data are expressed as the means ± standard deviations of experiments performed in triplicate. Significant differences were determined using one-way ANOVA, Tukey's multiple comparisons test. Differences were regarded as highly significant when $p < 0.0001$ (****). Bars: 20 μm.

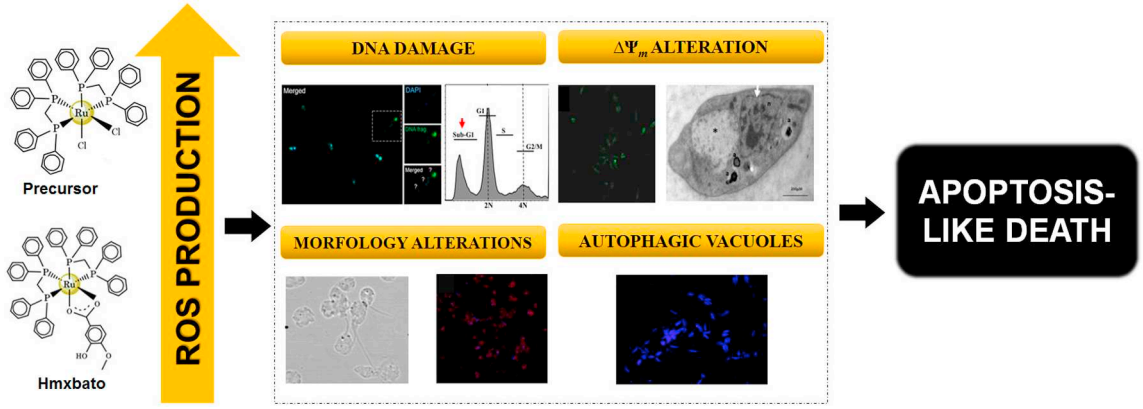

Fig. 9. Proposed mechanism of *L.* (*L.*) *amazonensis* death induced by ruthenium(II) complexes. Elevation of ROS induced depolarization in ($\Delta\Psi_m$); DNA cleavage; alterations in the parasite morphology and increased formation of autophagic vacuoles. These features together indicate that our complexes are inducing apoptosis-like death in *L.* (*L.*) *amazonensis* promastigotes.

presented DNA fragmentation. This effect was also produced by *Azadirachta* bioactive fractions against *L. donovani* promastigotes after treatment for 72 h. In addition, other result indicated parasite death by apoptosis [43], and similar effects were observed in *L. amazonensis* after treatment with 2 mM of hydrogen peroxide [40].

Mitochondrial dysfunctions produced by changes in $\Delta\Psi_m$ can be seen as a consequence of apoptosis or as an initial requirement for the occurrence of apoptosis [44]. The *Leishmania* parasite presents large and unique mitochondria, which is responsible for most of the energy supply, thus playing a critical role in the parasite's survival. This essential role of mitochondria makes them a potential target for the development of new therapeutic agents [45–47]. Some types of drugs or stress in trypanosomatids have been associated with the occurrence of alterations on $\Delta\Psi_m$ [48,49]. Our results indicate that both precursor and hmxbato were able to induce alterations in parasite mitochondria, leading to a depolarization of the ΔΨm at all times analyzed (24 and 48 h). However, the most significant alteration was observed after treatment with ruthenium complexes for 48 h, when both complexes presented $\Delta\Psi_m$ decreases of more than 75%. Luque-Ortega et al. [50] showed that *L. infantum* promastigotes exposed to benzophenone-derived bisphosphonium salts exhibited dissipation in $\Delta\Psi_m$ that was attributed to the compound's action on complex II of the respiratory chain. Moreover, $\Delta\Psi_m$ alterations in the *Leishmania* parasite are associated with augmented generation of ROS, which could result in

parasite death [42,51]. This would happen due to stress generation in the cell and consequent ROS formation resulting in lipid peroxidation that would influence the mitochondrial membrane fluidity causing the loss of $\Delta\Psi_m$ [24]. Additionally, it has already been demonstrated that respiratory chain inhibitors (complexes II and III) are associated with apoptosis occurrence in *Leishmania donovani* promastigotes [52]. In this work we demonstrated that both precursor and hmxbato significantly increased ROS generation after 24 h of treatment. These results support the hypothesis that ruthenium complexes may be causing apoptosis-like death among *L.* (*L.*) *amazonensis* promastigotes.

The autophagy process, which is marked by the formation of structures called autophagic vacuoles, is considered a cellular survival response. This process can be activated in situations involving cellular stress such as ROS production [53,54]. Low concentrations of ruthenium(II) complexes caused an increase in the formation of autophagic vacuoles in the parasite after 24 h of treatment, indicating that the autophagy process is being stimulated by complexes. This cell survival mechanism in promastigotes of the genus *Leishmania* has been produced by other compounds as demonstrated in a recent study using an innovative thiosemicarbazone molecule (4-nitro benzaldehyde thiosemicarbazone derived from S-(-)- limonene - BZTS) with miltefosine, a drug used in leishmaniasis treatment [32]. Similar results have also been recently reported for the compound C5 (*n*-benzyl 1-(4-methoxy)phenyl-9H-β-carboline-3-carboxamide) against *L.* (*L.*) *amazonensis* promastigotes. The C5 caused an elevation of ROS production, depolarization of the mitochondrial membrane, DNA fragmentation and an intense formation of autophagic vacuoles [27]. Chronic and/or unresolved stress can lead the cell to apoptotic events and consequently cell death [53]. We demonstrated through the increase of ROS that the ruthenium complexes produced a high-stress environment for the promastigotes. In response to this adverse environment and aiming to re-establish, parasite cells induced the formation of autophagic vacuoles. However, the response generated was probably insufficient, since apoptotic events occurred culminating with cell death.

Considering that cell death by apoptosis may involve biochemical processes and morphological changes, the next step was to analyze whether morphological changes also occurred due to treatment with ruthenium(II) complexes. Some morphological changes including cell shrinkage, as well as the loss of cell volume and plasma membrane integrity in a metazoan, are seen as markers of the apoptotic process [55,56]. The present work showed by morphological analysis that ruthenium(II) complexes at low concentrations, especially hmxbato, caused the cell shrinkage and loss of cell volume. Additionally, the round body shape presented by treated parasites and the strong labeling with phalloidin, especially with hmxbato treatment, indicate that the change in the actin polymerization pattern may be related to cell rounding. Ultrastructural analysis revealed intense mitochondrial swelling, increased numbers of acidocalcisomes, vacuoles and lipid bodies as well as an altered pattern of chromatin condensation. However, the cell membrane and kinetoplast remained intact. Nuclear and mitochondrial alterations are probably among the main factors underlying the potent anti-proliferative effect and the loss of viability in *Leishmania* species [57]. Acidocalcisomes, organelles whose features include acidic nature and high electron density, play a role in the storage of polyphosphates, calcium, magnesium and other elements [58]. Similar changes were observed in *L. amazonensis* promastigotes treated with 5 or 10 μM KH-TFMDI for 48 h [28].

Several studies have shown that the action of ruthenium complexes against tumor cells involves the induction of cellular death by apoptosis [21,59–61]. Li et al. [62] demonstrated that a ruthenium(II) polypyridyl complex denominated $[(L_1)_2RuL_2]\cdot 2ClO_4$ where L_1 = phen and L_2 = (2-trifloride-phenyl) imidazo[4,5-*f*][1,10]phenanthroline - o-TFPIP inhibited the proliferation and induced the apoptosis of a human liver cancer cell line (HepG2). Studies aiming to elucidate ruthenium-induced death mechanisms reveal that these complexes act through interactions with DNA, and may induce the generation of ROS [62,63]. Some similarities between the Trypanosomatidae family and tumor cell metabolisms have been observed since both exhibit high replication rates. Thus, both present a high energy demand [64]. The pro-apoptosis activity related to organometallic compounds was previously demonstrated for ruthenium(II) complexed with clotrimazole in *L.* (*L.*) *amazonensis* promastigotes through an experiment that demonstrated mitochondrial depolarization, DNA fragmentation, cell-cycle alteration profile and plasma membrane phospholipid externalization [39]. Therefore, the results demonstrated herein confirm the involvement of death by apoptosis in the action of ruthenium complexes on *L.* (*L.*) *amazonensis* parasites.

Considering that there are few studies in the literature aimed at elucidating the cytotoxic mechanism involved in the anti-parasite action of ruthenium complexes, the results presented herein will provide important knowledge on the action mechanism of this drug type. Our study describes, in an original research study, a probable mechanism of cell death whereby the hmxbato and precursor would be acting against *L.* (*L.*) *amazonensis* promastigotes.

The determination of the mechanism of death of a given molecule is only an initial step of the numerous steps for prospecting for a new drug. Stability studies are extremely important to verify the behavior molecular under different conditions, since a variety of factors may influence its stability. Thus, important tests such as (i) solubility studies, (ii) stability of the molecule in different solutions, (iii) degradation reactions and (iv) thermodynamic stability constitute a very important phase in this process [65,66]. For these reasons studies related to the stability of Hmxbato are part of our future prospects, as well as verifying anti-*Leishmania* action of this complex in an animal model by means of in vivo studies.

Abbreviations

AM160	[(*p*-cymene)$RuCl_2$(CTZ)]
AM162	[(*p*-cymene)RuCl(acac) (CTZ)]BF_4 (acac = acetylacetonate)
Bbato	cis-[Ru^{II}(η^2-$O_2CC_{10}H_{13}$)(dppm)$_2$]PF_6
BZTS	4-nitro benzaldehyde thiosemicarbazone derived from S-(-)-limonene
CM-H_2DCFDA	5-(and-6)-chloromethyl-2′,7′dichlorodihydrofluorescein diacetate, acetyl ester
CL	Cutaneous leishmaniasis
C5	*n*-benzyl 1-(4-methoxy)phenyl-9H-β-carboline-3-carboxamide
DAPI	4,6′-diamidino-2-phenylindole dilactate
DIC	Differential interference contrast
DMSO	Dimethyl sulfoxide
Dppm	bis(diphenylphosphino)methane
FBS	Fetal bovine serum
Hmxbato	cis-[Ru^{II}(η^2-$O_2CC_7H_7O_2$)(dppm)$_2$]PF_6
IC_{50}	50% inhibition concentration
KH-TFMDI	6,7-dichloro-3-[4-(trifluoromethyl)benzylidene] indolin-2-one
L. (*L.*) *amazonensis*	*Leishmania* (*Leishmania*) *amazonensis*
L. (*L.*) *infantum*	*Leishmania* (*Leishmania*) *infantum*
L. (*V.*) *braziliensis*	*Leishmania* (*Viannia*) *braziliensis*
LIT	Liver infusion tryptose
MCL	Mucocutaneous leishmaniasis
MDC	Monodansylcadaverine
Mtbato	cis-[Ru^{II}(η^2-$O_2CC_7H_7S$)(dppm)$_2$]PF_6
o-TFPIP	(2-trifloride-phenyl) imidazo[4,5-*f*][1,10]phenanthroline
Precursor	cis-[RuII(η^2-O_2CR)(dppm)$_2$]PF_6
PBS	Phosphate buffer saline
PI	Propidium iodide
PKDL	Post-kala-azar dermal leishmaniasis
ROS	Reactive oxygen species
Rh 123	Rhodamine 123

Salophen 4-acetamidofenil 2-hidroxibenzoato
TUNEL Terminal deoxynucleotidyl transferase dUTP nick end labeling
VOSalophen $[VO(C_{20}H_{16}N_4O_2]\cdot H_2O$
VL Visceral Leishmaniasis
WHO World Health Organization
$\Delta\Psi_m$ Mitochondrial membrane potential

Acknowledgments

We thank Dra. Ana Cláudia Arantes Marquez Pajuba from Immunology and Parasite Institute of the Federal University of Uberlândia (UFU) for helping with flow cytometric and the techniques Mariani Borges Franco and Rosiane Nascimento Alves from Institute of Cell Biology of the UFU for assistance with confocal microscopy and transmission electron microscopy.

This study was supported by Brazilian Agencies of Research: Conselho Nacional de Desenvolvimento Científico e Tecnológico (CNPq) (479000/2013-1); Coordenação de Aperfeiçoamento de Pessoal de Nível Superior (CAPES) (PNPD20131333-32006012006PO); Fundação de Amparo à Pesquisa do Estado de Minas Gerais (FAPEMIG) (APQ-01307-17, APQ-00376-10, APQ-01637-15); Fundação de Amparo à Pesquisa do Estado de São Paulo (FAPESP) - Center of Toxins, Immune Response and Cell Signaling (CeTICS): grant number: 2014/24170-5 and Nanobiotechnology INCT TeraNano-CNPq/CAPES/FAPEMIG, Grant numbers CNPq-465669/2014-0).

References

[1] World Health Organization, Leishmaniasis: Strengthening Cross-Border Collaboration for Control in Central Asian and Middle Eastern Countries of the WHO European and Eastern Mediterranean Regions: Report of a Bi-Regional Meeting, Turkmenbasi, Thurkmenistan, http://apps.who.int/iris/bitstream/10665/173803/1/9789241508780_eng.pdf?ua=1, (2014).
[2] World Health Organization, Weekly Epidemiological Record, Geneva, http://www.who.int/wer/, (2017).
[3] A.K. Haldar, P. Sen, S. Roy, Mol. Biol. Int. 11 (2011) 1–23, https://doi.org/10.4061/2011/571242.
[4] N. Singh, B.B. Mishra, S. Bajpai, R.K. Singh, V.K. Tiwari, Bioorg. Med. Chem. 22 (2014) 18–45, https://doi.org/10.1016/j.bmc.2013.11.048.
[5] A. Khamesipour, Expert. Opin. Biol. Ther. 14 (1641) (2014) 1649, https://doi.org/10.1517/14712598.2014.945415.
[6] M. Mital, Z. Ziora, Coord. Chem. Rev. (2018) 1–25, https://doi.org/10.1016/j.ccr.2018.02.013.
[7] M. Ravera, Elsa. Moreno-Viguri, R. Paucar, S. Peres-Silanes, E. Gabano, Eur. J. Med. Chem. (2018) 1–51, https://doi.org/10.1016/j.ejmech.2018.05.044.
[8] R.S. Correa, M.M. Da Silva, A.E. Graminha, C.S. Meira, J.A. Santos, D.R. Moreira, M.B. Soares, G. Von Poelhsitz, E.E. Castellano, C. Bloch Jr., M.R. Cominetti, A.A. Batista, J. Inorg. Biochem. 156 (2016) 153–163, https://doi.org/10.1016/j.jinorgbio.2015.12.024 (Epub 2016 Jan 2).
[9] X. Zhao, L. Li, G. Yu, S. Zhang, Y. Li, Q. Wu, X. Huang, W. Mei, Comput Struct Biotechnol J 17 (2019) 21–30, https://doi.org/10.1016/j.csbj.2018.11.010.
[10] J. Marques, A.M.S. Silva, M.P.M. Marques, S.S. Braga, Inorg. Chem. Commun. 488 (2019) 71–79, https://doi.org/10.1016/j.ica.2019.01.003.
[11] M. Fandzloch, J.M.M. Arriaga, M. Sánchez-Moreno, A. Wojtczak, J. Jezierska, J. Sitkowski, J. Wiśniewska, J.M. Salas, I. Łakomska, J. Inorg. Biochem. 176 (2017) 144–155, https://doi.org/10.1016/j.jinorgbio.2017.08.018.
[12] M.S. Costa, Y.G. Gonçalves, D.C.O. Nunes, D.R. Napolitano, P.I.S. Maia, R.S. Rodrigues, V.M. Rodrigues, G. Von Poelhsitz, K.A.G. Yoneyama, J. Inorg. Biochem. 175 (2017) 225–231, https://doi.org/10.1016/j.jinorgbio.2017.07.023.
[13] M. Pongratz, P. Schluga, M.A. Jakupec, V.B. Arion, C.G. Hartinger, G. Allmaier, B.K. Keppler, J. Anal. At. Spectrom. 19 (2004) 46–51, https://doi.org/10.1039/B309160K.
[14] J.C. Toledo, B.S. Lima Neto, D.W. Franco, Coord. Chem. Rev. 249 (2005) 419–431, https://doi.org/10.1016/j.ccr.2004.09.016.
[15] T. Chen, Y. Liu, W.J. Zheng, J. Liu, Y.S. Wong, Inorg. Chem. 49 (2010) 6366–6368, https://doi.org/10.1021/ic100277w.
[16] J. Shen, H.C. Kim, J. Wolfram, C. Mu, W. Zhang, H. Liu, Y. Xie, J. Mai, H. Zhang, Z. Li, M. Guevara, Z. W Mao, H. Shen, Nano Lett. 17 (2017) 2913 – 2920. doi:https://doi.org/10.1021/acs.nanolett.7b00132.
[17] J. Williamson, T.J. Scott-Finnigan, Antimicrob. Agents Chemother. 13 (1978) 735–744, https://doi.org/10.1128/AAC.13.5.735.
[18] N.P. Farrell, J. Williamson, D.J.M. McLaren, Biochem. Pharmacol., 33 (1984) 961–971. doi:https://doi.org/10.1016/0006-2952(84)90501-X.
[19] R.A. Sanchez-Delgado, A. Anzellotti, Mini-Rev. Med. Chem. 4 (2004) 23–30, https://doi.org/10.2174/1389557043487493.
[20] C.G. Hartinger, M.A. Jakupec, S. Zorbas-Seifried, M. Groessl, A. Egger, W. Berger, H. Zorbas, P.J. Dyson, B.K. Keppler, Chem. Biodivers. 5 (2008) 40–55, https://doi.org/10.1002/cbdv.200890195.
[21] K. Zheng, Q. Wu, C. Wang, W. Tan, W. Mei, Anti Cancer Agents Med. Chem. 17 (2017) 29–39, https://doi.org/10.2174/1871520616666160622085441.
[22] C. Irace, G. Misso, A. Capuozzo, M. Piccolo, C. Riccardi, A. Luchini, M. Caraglia, L. Paduano, D. Montesarchio, R. Santamaria, Sci. Rep. 28 (2017) 1–13, https://doi.org/10.1038/srep4536.
[23] A. Debrabant, N. Lee, S. Bertholet, R. Duncan, H.L. Nakhasi, Int. J. Parasitol. 33 (2003) 257–267, https://doi.org/10.1016/S00207519(03)00008-0.
[24] D. Smirlis, M. Duszenko, A.J. Ruiz, E. Scoulica, P. Bastien, N. Fasel, Parasit. Vectors 3 (2010) 1–15, https://doi.org/10.1186/1756-3305-3-107.
[25] M. Deponte, Biochim. Biophys. Acta. 1783 (2008) 1996–1405. doi:https://doi.org/10.1016/j.bbamcr.2008.01.018.
[26] F.A. Marinho, K.C.S. Gonçalves, S.S. Oliveira, A.S.C. Oliveira, M. Bellio, C.M. d'Avila-Levy, A.L. Santos, M.H. Branquinha, Mem. Inst. Oswaldo Cruz 106 (2011) 507–509, https://doi.org/10.1590/S0074-0276.
[27] E.A. Mendes, V.C. Desoti, S.O. Silva, T. Ueda-Nakamura, B.P.D. Filho, S.F. Yamada-Ogatta, Chem. Biol. Interact. 256 (2016) 16–24, https://doi.org/10.1016/j.cbi.2016.06.018.
[28] B.R.F. Verçoza, J.L.P. Godinho, S.T. de Macedo-Silva, K. Huber, F. Bracher, W. de Souza, J.C.F. Rodrigues, Apoptosis. 22 (2017) 1169–1188.doi:https://doi.org/10.1007/s10495-017-1397-8.
[29] I. S. Chauhana, G. S. Raob, J. Shankarc, L. K. S. Chauhanc, G. J. Kapadiad, N. Singha, 67 (2018) 627 – 636. doi:https://doi.org/10.1016/j.parint.2018.06.004.
[30] B.P. Sullivan, T.J. Meyer, Inorg. Chem. 21 (1982) 1037–1040, https://doi.org/10.1021/ic00133a033.
[31] F.A. Marinho, K.C.S. Gonçalves, S.S.C. Oliveira, D.S. Gonçalves, F.P. Matteoli, S.H. Seabra, A.C. Oliveira, M. Bellio, S.S. Oliveira, T. Souto-Padrón, C.M. d'Avila-Levy, A.L. Santos, M.H. Branquinha, PLoS One. 9 (2014) 1–11. doi:https://doi.org/10.1371/journal.pone.0087659.
[32] D.B. Scariot, E.A. Britta, A.L. Moreira, H. Falzirolli, C.C. Silva, T. Ueda-Nakamura, B.P. Dias-Filho, C.V. Nakamura, Front. Microbiol. 8 (2017) 1–16, https://doi.org/10.3389/fmicb.2017.00255.
[33] E.S. Coimbra, L.M.R. Antinarelli, N.P. Silva, I.O. Souza, R.S. Meinel, M.N. Rocha, Chem. Biol. Interact. 260 (2016) 50–57, https://doi.org/10.1016/j.cbi.2016.10.017.
[34] P.A. Machado, J.O.F. Morais, G.S.G. Carvalho, W.P. Lima, G.C. Macedo, E.A. Britta, C.V. Nakamura, A.D. da Silva, A. Cuin, E.S. Coimbra, J. Biol. Inorg. Chem. 22 (2017) 929–939, https://doi.org/10.1007/s00775-017-1471-2.
[35] D. Gambino, L. Otero, Inorganica Chim. Acta (2017) 1–63, https://doi.org/10.1016/j.ica.2017.07.068.
[36] D.C.O. Nunes, L.B. Bispo-da-Silva, D.R. Napolitano, M.S. Costa, M.M.N.R. Figueira, R.S. Rodrigues, V.M. Rodrigues, K.A.G. Yoneyama, PLoS One. 12 (2017) 1–10. doi:https://doi.org/10.1371/journal.pone.0180530.
[37] A.B. Caballero, A. Rodríguez-Diéguez, M. Quirós, J.M. Salas, Ó. Huertas, I. Ramírez-Macías, F. Olmo, C. Marín, G. Chaves-Lemaur, R. Gutierrez-Sánchez, M. Sánchez-Moreno, Eur. J. Med. Chem. 85 (2014) 526–534, https://doi.org/10.1016/j.ejmech.2014.08.026.
[38] S. Chowdhury, T. Mukherjee, R. Mukhopadhyay, B. Mukherjee, S. Sengupta, S. Chattopadhyay, P. Jaisankar, S. Roy, H.K. Majumder, EMBO Mol. Med. 4 (2012) 1126–1143, https://doi.org/10.1002/emmm.201201316.
[39] E. Iniguez, A. Varela-Ramirez, A. Martinez, C.L. Torres, R.A. Sanchez-Delgado, R.A. Maldonado, Acta Trop. 164 (2016) 1–30, https://doi.org/10.1016/j.actatropica.2016.09.029.
[40] M.S. Da Silva, M. Segatto, R.S. Pavani, F. Gutierrez-Rodrigues, V. da Silva Bispo, M.H.G. de Medeiros, R.T. Calado, M.C. Elias, M.I.N. Cano, Biochim. Biophys. Acta 1864 (2017) 138–150, https://doi.org/10.1016/j.bbamcr.2016.11.001.
[41] S.E. Reece, L.C. Pollitt, N. Colegrave, A. Gardner, PLoS Pathog. 7 (2011) 1–9, https://doi.org/10.1371/journal.ppat.1002320.
[42] M. Shadab, B. Jha, M. Asad, M. Deepthi, M. Kamran, N. Ali, PLoS One. 12 (2017) 1–31. doi:https://doi.org/10.1371/journal.pone.0171306.
[43] G. Chouhan, M. Islamuddin, M.Y. Want, H.A. Ozbak, H.A. Hemeg, D. Sahal, F. Afrin, Front. Microbiol. 6 (2015) 1–19, https://doi.org/10.3389/fmicb.2015.01368.
[44] E. Gottlieb, S.M. Armour, M.H. Harris, C.B. Thompson, Cell Death Differ. 10 (2003) 709–717, https://doi.org/10.1038/sj.cdd.4401231.
[45] D.R. Green, J.C. Reed, Science. 28 (1998) 1309–1312. doi:https://doi.org/10.1126/science.281.5381.1309.
[46] W. De Souza, M. Attias, J.C.F. Rodrigues, Int. J. Biochem. Cell Biol. 41 (2009) 2069–2080, https://doi.org/10.1016/j.biocel.2009.04.007.
[47] M. Kathuria, A. Bhattacharjee, K.V. Sashidhara, S.P. Singh, K. Mitra, Antimicrob. Agents Chemother. 58 (2014) 5916–5938, https://doi.org/10.1128/AAC.02459-14.
[48] J.F. Alzate, A.A. Arias, D. Moreno-Mateos, A. Alvarez-Barrientos, A. Jimenez-Ruiz, Mol. Biochem. Parasitol. 152 (2007) 192–202, https://doi.org/10.1016/j.molbiopara.2007.01.006.
[49] G.A. Ribeiro, E.F. Cunha-Junior, R.O. Pinheiro, S.A. da-Silva, M.M. Canto-Cavalheiro, A.J. da Silva, P.R. Costa, C.D. Netto, R.C. Melo, E.E. Almeida-Amaral, E.C. Torres-Santos, J. Antimicrob. Chemother. 68 (2013) 789–799, https://doi.org/10.1093/jac/dks498.
[50] J.R. Luque-Ortega, P. Reuther, L. Rivas, C. Dardonville, J. Med. Chem. 53 (2010) 1788–1798, https://doi.org/10.1021/jm901677h.
[51] L.M. Antinarelli, R.M. Dias, I.O. Souza, W.P. Lima, J. Gameiro, A.D. Da Silva, Chem. Biol. Drug Des. 84 (2015) 704–714, https://doi.org/10.1111/cbdd.12540.
[52] A. Mehta, C. Shaha, J. Biol. Chem. 279 (2004) 11798–11813, https://doi.org/10.1074/jbc.M309341200.
[53] S. Dolai1, S. Adak, Mol. Biochem. Parasitol. 197 (2014) 1–8, https://doi.org/10.

1016/j.molbiopara.2014.09.002.
[54] Z. Su, Z. Yang, Y. Xu, Y. Chen, Q. Yu, Mol. Cancer 14 (2015) 14–48, https://doi.org/10.1186/s12943-015-0321-5.14-48.
[55] G. Kroemer, L. Galluzzi, P. Vandenabeele, J. Abrams, E.S. Alnemri, E.H. Baehrecke, M.V. Blagosklonny, W.S. El-Deiry, P. Golstein, D.R. Green, M. Hengartner, R.A. Knight, S. Kumar, S.A. Lipton, W. Malorni, G. Nuñez, M.E. Peter, J. Tschopp, J. Yuan, M. Piacentini, B. Zhivotovsky, G. Melino, Cell Death Differ. 16 (2009) 3–11, https://doi.org/10.1038/cdd.2008.150.
[56] S. Gannavaram, A. Debrabant, Front. Cell. Infect. Microbiol. 2 (2012) 1–9, https://doi.org/10.3389/fcimb.2012.00095.
[57] E. Ledezma, A. Jorquera, H. Bendezú, J. Vivas, G. Pérez, Parasitol. Res. 88 (2002) 748–753, https://doi.org/10.1007/s00436-002-0649-9.
[58] S.N. Moreno, R. Docampo, J. Eukaryot. Microbiol. 56 (2009) 208–213, https://doi.org/10.1111/j.1550-7408.2009.00404.x.
[59] R. Pettinari, C. Pettinari, F. Marchetti, B.W. Skelton, A.H. White, L. Bonfili, J. Med. Chem. 57 (2014) 4532–4542, https://doi.org/10.1021/jm500458c.
[60] Q. Yu, Y. Liu, L. Xu, C. Zheng, F. Le, X. Qin, Y. Liu, J. Liu, Eur. J. Med. Chem. 82 (2014) 82–95, https://doi.org/10.1016/j.ejmech.2014.05.040.
[61] Z. Zhang, Q. Wu, X.H. Wu, F.Y. Sun, L.M. Chen, J.C. Chen, S.L. Yang, W.J. Mei, Eur. J. Med. Chem. 80 (2014) 316–324, https://doi.org/10.1016/j.ejmech.2014.04.070.
[62] Y. Li, Q. Wu, G. Yu, L. Li, X. Zhao, X. Huang, W. Mei, Eur. J. Med. Chem. (2018), https://doi.org/10.1016/j.ejmech.2018.12.041.
[63] V. Brabec, J. Kasparkova, Coordin. Chem. Rev 376 (2018) 75–94, https://doi.org/10.1016/j.ccr.2018.07.012.
[64] P. Borst, Trans. R. Soc. of Trop. Med. Hyg. 71 (1977) 3–4.
[65] A.K. Aggarwal, M. Gupta, Drug Dev. Ind. Pharm. 38 (2012) 1319–1327, https://doi.org/10.3109/03639045.2011.650644.
[66] S. Bajaj, D. Singla, N. Sakhuja, JAPS, 3 (2012) 129 – 138. doi:https://doi.org/10.7324/JAPS.2012.2322.